World Cancer Research Journal

WCRJ 2025; 12 : e2870
DOI: 10.32113/wcrj_20255_2870

THE VITAL ROLE OF TRPM2 IN BREAST CANCER CELL PROLIFERATION AND ITS DIFFERENCE IN EXPRESSION BETWEEN NON-HISPANIC WHITE AND NON-HISPANIC BLACK FEMALES

L.-P. HUANG[1], Y. LU[2], M. LI[3]

• • •

[1]Immunology & Transplant Science Center, Houston Methodist Research Institute, Houston, TX, USA
[2]Center for Aging, School of Medicine, Tulane University, New Orleans, LA, USA
[3]Department of Physiology, Tulane University Health Sciences Center, New Orleans, LA, USA

Corresponding Author
Ming Li, Ph.D; e-mail: mli@tulane.edu

ABSTRACT – ***Objective:*** To study the racial disparity of transient receptor potential melastatin-related channel subtype 2 (TRPM2) expression in non-Hispanic black (NHB) women and non-Hispanic white women (NHW) breast cancer tissues. Specific roles of TRPM2 in the proliferation and apoptosis of the human mitogenic breast cancer cells (MCF-7 ER+) are also investigated.

Materials and Methods: TRPM2 expression analysis was performed using the normalized mRNA expression data downloaded from Broad GDAC Firehose. The functions of TRPM2 in normal and cancer cells are revealed using patch-clamp recording and intracellular calcium imaging techniques.

Results: TRPM2 is expressed at different levels in breast ductal and lobular neoplasm disease between NHB and NHW. Selective knock-down of TRPM2 mRNA with small interfering RNA (siRNA/TRPM2) caused substantial inhibition of cell proliferation of MCF-7(ER+) cells but not in the control human mammary epithelial (HME) cells. The siRNA/TRPM2 also induced cellular apoptosis in MCF-7(ER+) cells but not HME cells. Immunofluorescent staining shows that TRPM2 abnormally localizes in the MCF-7(ER+) nuclei but not HME cells.

Conclusions: These results suggest that TRPM2 is essential in promoting MCF-7(ER+) cell proliferation and may be a potential target for breast cancer treatment.

KEYWORDS: TRPM2, Racial disparity, Cell proliferation, Calcium signal, Breast cancer

LIST OF ABBREVIATIONS: NHB: Non-Hispanic Black; NHW: Non-Hispanic White; GAPDH: Glyceraldehyde phosphate-3-dehydrogenase; IP_3R: Inositol 1,4,5-trisphosphate receptor; NAD: Nicotinamide adenine dinucleotide; PCR: Polymerase chain reaction; siRNA: Small interfering RNA; TRPM2: Transient receptor potential melastatin-related channel subtype 2; TUNEL: Terminal deoxynucleotidyl transferase biotin-dUTP nick end labeling; PARP: Poly(ADP-ribose) polymerase; MTT: [3-(4,5-dimethylthiazol-2-yl)-2,5-diphenyltetrazolium bromide] assay; HMEC: Human mammary epithelial cell; MCF-7: Michigan Cancer Foundation-7; HATS: Histone acetyltransferases.

INTRODUCTION

In the United States, the incidence of breast cancer is lower in non-Hispanic Black (NHB) women than in non-Hispanic whites (NHW). However, the mortality rate is paradoxically higher for NHB women[1]. Such racial disparity is partially due to more aggressive breast cancer patients being screened out in NHB women than in NHW[2]. Many research efforts have been spent addressing such racial disparity issues; however, these efforts are limited by a lack of knowledge of the mechanism underlying the racial disparity and the valuable biomarkers that can be used to study the mechanism[3]. Searching for selective therapeutic targets with apparent genetic expression differences between NHB and NHW cancer patients is emergent.

Transient receptor potential melastatin-related channel 2 (TRPM2), has been shown to be closely related to cancer cell proliferation and migration[4-6]. An unusual cellular expression pattern has recently been reported in several types of malignant tumors, including prostate, breast, and tongue cancer cells, in which TRPM2 is overexpressed in cancer cells and located abnormally in the cytoplasm and the nucleus[7-10]. We are particularly interested in exploring racial disparity in TRPM2 gene expression between NHB and NHW breast cancer patients. Furthermore, the functional deviations of the TRPM2 channel related to nucleus relocation in breast cancer cells are being investigated.

TRPM2 functions as a Ca^{2+} entry channel[4,7-12], which can be activated by ADP-ribose[13], β-nicotinamide adenine dinucleotide (β-NAD)/H_2O_2[13], TNFα[14], or calmodulin[14], increasing the intracellular free calcium concentration $[Ca^{2+}]_i$[15]. ADP-ribose is a known breakdown product of NAD[16], cADP-ribose[17], and protein deacetylation[16,18]. The Nudix region of TRPM2 functions as the binding site for the ADP-ribose[17]. In the nucleus, ADP-ribose is converted into poly(ADP-ribose) by poly(ADP-ribose) polymerase (PARP), which plays a vital role in DNA repair[19-21] and cell replication[22-24]. Over-activation of PARP can cause cell death due to the depletion of the cytoplasmic ATP[25,26]. The opening of TRPM2 channels in response to oxidative stress is associated with the activation of the PARP[27-30]. Furthermore, it has been demonstrated that TRPM2 mediates oxidative stress-induced cell death by activating PARP cleavage[31].

MATERIALS AND METHODS

TRPM2 Expression Analysis: The normalized mRNA expression data was downloaded from Broad GDAC Firehose (The Cancer Genome Atlas homepage https://www.cancer.gov/ccg/). The patients' clinic data, including race/ethnicity, gender, survival information, case ID, primary site, project, and disease type, were downloaded from the GDC Data portal. Up to February 21st. 2022, 778 ductal and lobular neoplasms female patients were retrieved, including 157 NHB and 621 NHW. The survivors are 646, and the deceased are 132. Python 3.7.6 was used for data processing, and SciPy v1.8.0 was loaded for a one-side *t*-test. The *p*-value was set as <0.05 as significant.

Cell Culture: This study used two breast epithelial cell lines: a human breast adenocarcinoma cell line, MCF-7(ERα^+) (ATCC, Rockville, MD, USA), and a non-mitogenic mammary epithelial cell line (HMEC, Clonetics, San Diego, CA, USA). MCF-7(ERα^+) cells were cultured in Minimum Essential Medium (Eagle) with 2 mM L-glutamine and Earle's BSS adjusted to contain 1.5 g/L sodium bicarbonate, 0.1 mM non-essential amino acids and 1 mM sodium pyruvate and supplemented with 0.01 mg/ml bovine insulin, 10% fetal bovine serum, 100 U/ml penicillin and 100 μg/ml streptomycin (P/S). HME cells were cultured in Mammary Epithelial Growth Medium (MEGM), serum-free, supplemented with 100 ng/ml cholera toxin. All cells were maintained in a humidified atmosphere of 5% CO_2 at 37°C. Cultural media was replaced every 2-5 days. After cells were grown to confluence, they were treated with trypsin and 1 mM EDTA for 5 min (diluted, 1:3) and re-plated on 75 cm^2 or 35 cm^2 culture dishes.

Western Blot Analysis: Nuclei were isolated from MCF-7(ER+) and HMEC for nuclear protein extraction using CelLytic™ NucLEAR™ Extraction Kit (Sigma-Aldrich, Inc. St. Louis, MO, USA). The nuclei were then lysed, and protein concentration was determined using a BCA reagent (Pierce Chemical Co., Rockford, IL, USA). Equal amounts of protein extracts (50 μg) were separated in SDS-PAGE gels (Bio-RAD Laboratories, Hercules, CA, USA). The proteins were transferred electrophoretically to a 0.2 μm nitrocellulose membrane. At room temperature, 5% non-fat dry milk in PBS containing 0.1% Tween 20 (PBS-T) was used as a blocking agent for 1 hour. The membrane was then treated with 1:300 dilution of TRPM2 primary antibody (Bethyl Laboratories, Inc., Montgomery, TX, USA) at 4°C overnight, rinsed briefly using three changes of PBS-T, and further incubated with HRP-conjugated secondary antibody (dilution 1:2000 in PBS-T) for 1 hour at room temperature with constant agitation. The film was developed with the ECL Western blot detection reagent kit (Amersham Pharmacia Biotech, Piscataway, NJ, USA).

RT-PCR: RNA was extracted from both cell lines using TRI-REAGENT® (Molecular Research Center, Inc., Cincinnati, OH, USA). A 2 μg sample of total RNA from each cell line was incubated with 1 unit of RNase-free DNase for 10 minutes at 37˚C and then at 65˚C for another 10 minutes. Random primers (1 μg) were added, and the tube was kept at 70˚C for 5 minutes. Subsequently, 5 μl of M-MLV reverse transcriptase reaction buffer (5x), 1 μl of 10 mM PCR nucleotide mix, 25 units of rRNasin® RNase inhibitor, and 200 units of M-MLV reverse transcriptase were added to the tube and incubated at 37˚C for 1 hour. All reagents were purchased from Promega Co. (Madison, WI, USA). The cDNA product (2 μl) was mixed with 1.5 units TaKaRa Taq™, 2.5 μl 10x PCR buffer, 2 μl 2.5 mM dNTP mixture (TaKaRa Shuzo Co., Otsu, Japan), and 100 pM of each primer. The final volume of each tube was adjusted to 25 μl with DEPC water. The amplification protocol for PCR was set as follows: 94˚C for 4 minutes, followed by 30 cycles of amplification steps (i.e., 94˚C for 2 min, 60˚C for 30 sec, 72˚C for 40 sec), and the final extension at 72˚C for 8 minutes. PCR products were analyzed using agarose gel (1.5%) electrophoresis and visualized under UV light after staining with ethidium bromide (1 μg/ml).

Immunofluorescent Confocal Microscopy: Cells were placed in chamber slides for 1 day, allowing attachment. Cells were washed 3 times with PBS, fixed with methanol at RT for 5 minutes, and permeabilized in 0.1% Triton X-100 in PBS for 30 minutes. After treatment with 5% goat serum for 10 minutes, cells were incubated with the primary antibody (rabbit anti-TRPM2, 1:50, Bethyl Laboratories, Inc., Montgomery, TX, USA) for 2 h at room temperature, followed by the secondary antibody (goat anti-rabbit IgG FITC conjugated, 1:200, Bethyl Laboratories, Inc., Montgomery, TX, USA) for 30 minutes in a dark room. Propidium iodide (PI) (Abcam Inc., Cambridge, MA, USA) was used for nuclear staining. Confocal microscopy was performed using a Leica TCS SP2 confocal microscope equipped with five lasers, including the Argon 488 nm and HeNe 543 nm (Leica Microsystems, Exton, PA, USA).

Small interfering RNA (siRNA): Cells were cultured on 96-well microplates at approximately 33% confluence and transfected with 100 pM either siRNA specific to TRPM2 (5'-AUAGAUCAGGAACUCCGUCUC-3') or scrambled siRNA (Integrated DNA Technology, Coralville, IA, USA) using Lipofectamine™ 2000 transfection reagent (Invitrogen, Carlsbad, CA, USA). Cell proliferation was monitored by a 2-(2-methoxy-4-nitrophenyl)-3-(4-nitrophenyl)-5-(2,4-disulfophonyl)-2H-tetrazolium (WST-8) cell counting kit (Alexis Biochemicals Corp, San Diego, CA, USA) according to manufacturers' instructions.

Apoptosis was assessed using a TUNEL assay (Apoptag®Fluorescin Direct *In Situ* Apoptosis Detection Kit, Chemicon, S7160, Temecula, CA, USA) according to the manufacturer's instructions. The nuclei of the cells were stained with propidium iodide. Briefly, MCF-7(ERα^+) and HME cells were plated at ~50 percent confluence and allowed to grow for 24 hours. Cells were treated with siRNA/TRPM2 or scrambled siRNA/TRPM2 for 48 hours and then subjected to the TUNEL assay.

Patch clamp electrophysiology. The activity of TRPM2 was examined by using whole-cell patch clamp recordings. Recordings were carried out using gigaseal whole-cell patch methods. Pipette resistance was in the range of 2-5 MΩ in our intracellular pipette solutions. An EPC-9 patch clamp amplifier (HEKA, Gottingen, Germany) filtered at 2.9 kHz was used, and data were acquired using Pulse/PulseFit software (HEKA, HEKA, Gottingen, Germany). Voltage-dependent currents were corrected for linear leak and residual capacitance using an online P/n subtraction. Following whole-cell access, the cells were held at 0 mV with test pulses ranging from -80 to 80 mV in 10 mV increments. Extracellular bath solutions contained (in mM): 140 NaCl, 1.2 $MgCl_2$, 1.2 $CaCl_2$, 4KCl, 10 HEPES, pH 7.4 (CsOH). The pipette solution contained 145 Cs-glutamate, 8 NaCl, 2 $MgCl_2$, 10 Cs-EGTA, 10 HEPES, pH 7.2 (CsOH). In HMEC and MCF-7(ERα^+) cells, 300 μM ADP-ribose was included in the pipette solution.

Calcium imaging. MCF-7(ERα^+) and HME cells were plated onto 25-mm glass coverslips (Fisher, Pittsburgh, PA, USA). Cytosolic Ca^{2+} concentration was estimated using the Ca^{2+}-sensitive fluorophore Fura-2 (Cat# F-1201; Molecular Probes, Eugene, OR, USA). The measurement solution contained (in mM): 130 NaCl, 5 KCl, 1.28 $CaCl_2$, 1.2 $MgCl_2$, 25 HEPES, pH to 7.4 with NaOH. Cells were incubated with Fura 2-AM for 30 min (37˚C in 5% CO_2 in the humidified atmosphere) in a loading solution that contained the measurement solution plus 3 μM Fura 2-AM and 3 μl of a 10% pluronic acid solution. After Fura-2 loading, cells were washed twice and incubated in a Fura-free measurement solution for de-esterification for an additional 20 min. H_2O_2 (300 μM) was used to induce TRPM2-mediated calcium influx. Experiments were carried out using an inverted microscope with a 175-W Xenon arc lamp Metafluor Imaging System (Nikon Instrument, Lewisville, TX, USA). A computer-driven filter wheel-controlled switching of excitation wavelengths (340 and 380 nm). The emitting fluorescent signal (510 nm) was acquired by an ADC 20 MHz camera (Photometrics Coolsnap FX Monochrome, Nikon, Lewisville, TX, USA). Acquisition time per image was 250 ms, and the empirical K_d obtained for Ca^{2+} binding to Fura-2 in our system was 269 nM. Data were acquired using MetaFluor 5.0R3 on an OEI (Konica, Ramsey, NJ, USA) P4 1400 MHz processor with 1-GB RAM using Windows 2000 Professional SP3.

RESULTS

TRPM2 mRNA expression is significantly higher in NHB than in NHW breast cancer patients

The normalized mean mRNA expression level is 562.61 ± 33.51 in ductal and lobular neoplasms of NHB women and 344.16 ± 10.94 in NHW women, respectively (series cut-off 3.6 e^{-9}, Figure 1A). In the survivor group, the mean TRPM2 mRNA expression in NHB and NHW women are 559.51 ± 35.94 and 351.79 ± 12.44, respectively (series cut-off 2.07 e^{-7}, Figure 1B). TRPM2 mRNA expression in NHB and NHW women in the deceased group is 576.25 ± 87.96 and 317.30 ± 22.84, respectively (p = 0.01, Figure 1C).

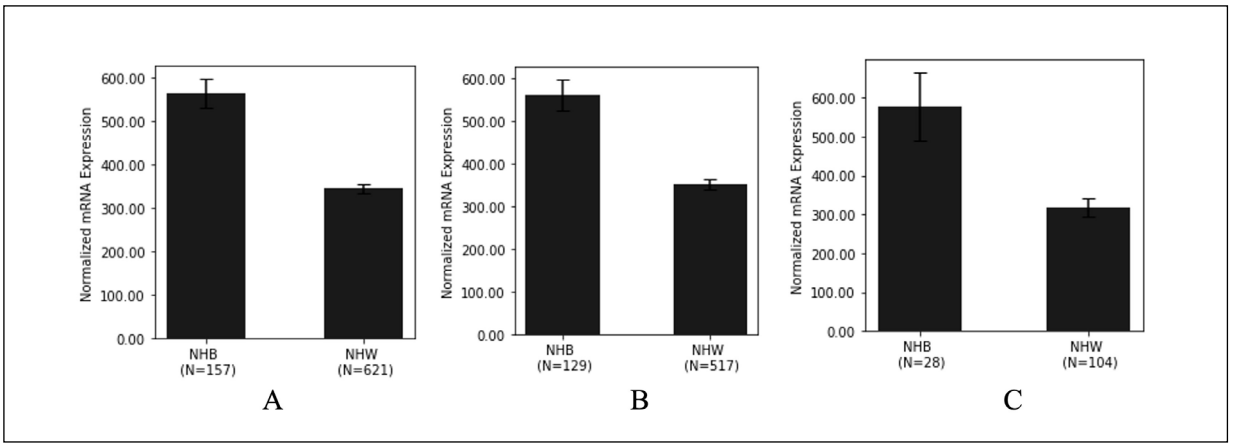

Figure 1. TRPM2 mRNA expression in breast cancer (ductal and lobular neoplasms) of Non-Hispanic Black (NHB) and Non-Hispanic White (NHW) female patients. *A*, TRPM2 mRNA expression in breast cancer patients of NHB (n = 157) and NHW (n = 621). *B*, TRPM2 mRNA expression in breast cancer survivors of NHB (n = 129) and NHW (n = 517). *C*, TRPM2 mRNA expression in the deceased breast cancer of NHB (n = 28) and NHW (n = 104).

TRPM2 Expression in MCF-7(ERa$^+$) Cancer Cells

To confirm the presence of TRPM2 expression in MCF-7(ERα^+) and HME cells, RT-PCR was used to evaluate TRPM2 mRNA expression in both cell types. As shown in Figure 2A, TRPM2 mRNA is detected in both cell lines, showing a clear PCR product at approximately 200 bp.

After confirming the expression of the TRPM2 message, we then investigated the expression and distribution of the TRPM2 proteins in both cell types using Western blot analysis. Figure 2B shows that TRPM2 is expressed in both MCF-7(ERα^+) and HMEC whole cell fractions, revealed by antibodies targeting TRPM2. Furthermore, TRPM2 was significantly expressed in or proximal to the nuclear fraction of MCF-7(ERα^+) cells but not in HME cell nuclear fractions.

A closer look at the sub-cellular distribution of TRPM2 proteins using confocal microscopy revealed similar results. The subcellular distribution of TRPM2 in HMECs was near the plasma membrane and throughout the cytoplasm. However, in MCF-7(ERα^+) cells, as indicated with the white arrow in Figure 2C, TRPM2 is highly expressed in the nuclear region of MCF-7(ERα^+) cells. These data reveal a distict expression pattern of the TRPM2 protein in these cancer cells, absent in non-cancer ones.

Functional Expression of TRPM2

Next, we investigated whether the differential expression translated into altered functionality of these proteins in the two different cell types. Using whole-cell patch clamp and fura-2 calcium imaging methods, we were able to determine the functionality of these proteins in these cells. Figure 3 (A, B, D, E) represents typical current traces from whole-cell patch experiments. In these experiments, ADP-ribose

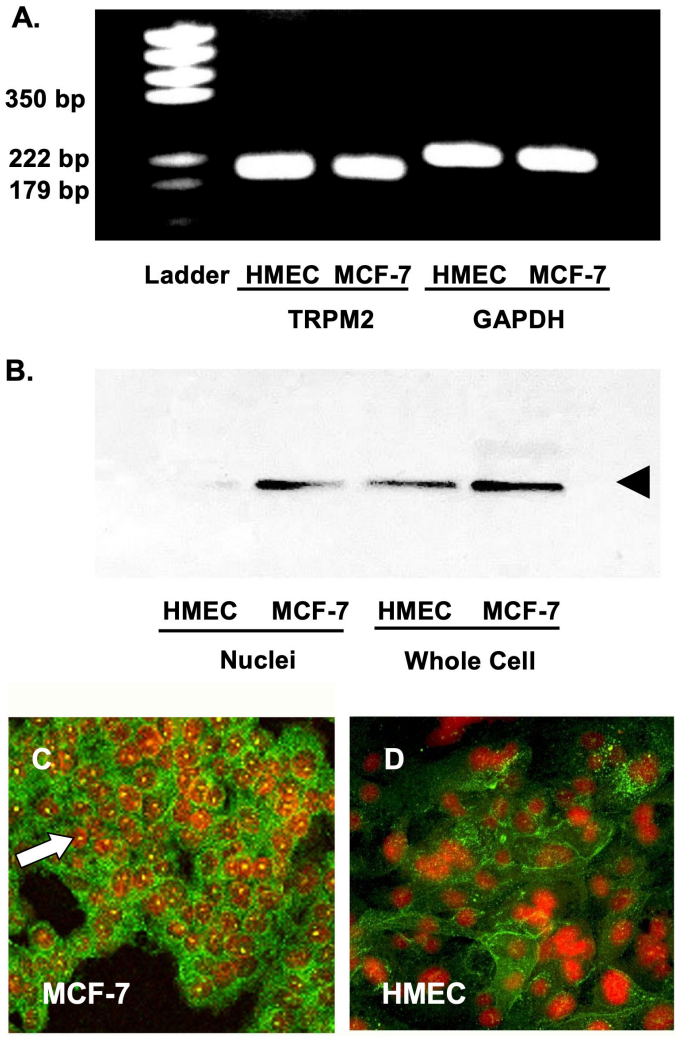

Figure 2. *A*, RT-PCR analysis of TRPM2 in MCF-7(ERα⁺) cells (MCF-7) and HME cells. TRPM2 bands ~ 200 bp. *B*, Western Blot analysis of TRPM2 in MCF-7(ERα⁺) and HME cells. Nuclei preparation *vs*. whole cell preparations. The arrow indicates TRPM2 staining. *C* and *D*, Confocal microscopy show the subcellular expression of TRPM2 protein in MCF-7(ERα⁺) and HME cells, respectively. Red represents Propidium iodide nuclei staining; Green represents FITC conjugated secondary antibody against TRPM2. Arrows indicate the nuclear localization of TRPM2. Images are the mid-section of the z-series images (30 images).

(300 μM) induced calcium current in HME cells (Figure 3B) was significantly larger than the current induced in MCF-7(ERα⁺) cells (Figure 3E) under the same conditions. The current-voltage (I/V) plots (Figure 3C (HMEC) and 3F (MCF-7(ERα⁺)) of these currents showed a slight rectification, which was also observed previously by others using the same recording conditions[14]. Figure 3G represents peak current density (pA/pF) for ADP-ribose-induced current in both cell types. The current density for HME cells was significantly higher than that of MCF-7(ERα⁺) cells.

Fura-2 fluorescent dye was used to measure intracellular calcium changes induced by oxidative stress. Oxidative stress was induced by treatment with H_2O_2 in both HMEC and MCF-7(ERα⁺) cells. Figure 4 shows typical calcium influx traces (4A, 4B) and compiled data from H_2O_2-induced calcium entry experiments. As shown in Figure 4C, basal calcium was ~75 nM in HME cells and ~90 nM in MCF-7(ERα⁺) cells. After applying H_2O_2 (100 μM), intracellular calcium was significantly increased to ~140 nM in HME cells. However, H_2O_2-induced calcium influx was substantially lower under similar conditions in MCF-7(ER+) cells. These data were consistent with the patch-clamp data, suggesting decreased calcium influx from TRPM2 in cancer cells.

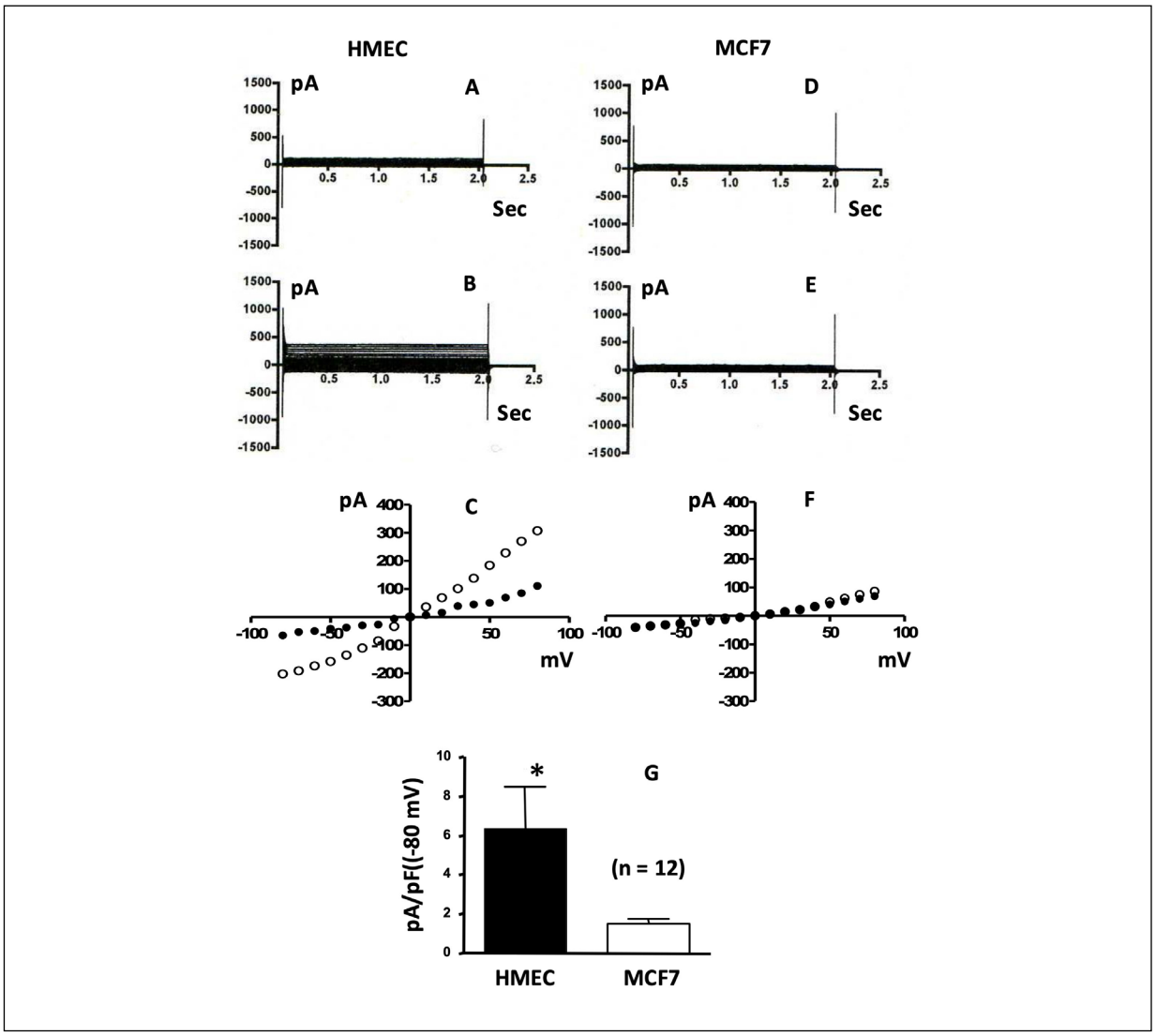

Figure 3. ADP-ribose induced cation current in HME cells (*A*, *B*) and MCF-7(ERα$^+$) cells (*D*, *E*). *A* and *D* show currents at 1 min after breaking in. *B* and *E* show currents after 10 min after breaking in. *C* and *F* displace current-voltage plots. Solid circles represent data from *A* and *D*; Open circles represent data from *B* and *E*. Panel *G* represents pooled current densities recorded at -80 mV. n = 12, * = $p < 0.01$.

To verify TRPM2's role in H_2O_2-induced calcium influx in HME cells, we used siRNA targeted against TRPM2 (siRNA/TRPM2, 100 pM) to inhibit TRPM2 expression. Figure 4D shows no calcium influx was observed in these cells after treatment with siRNA/TRPM2. The siRNA efficiencies in both cell types were confirmed, as shown in Figure 4E. These data suggest that TRPM2 is responsible for H_2O_2-induced calcium influx in HME cells but not in MCF-7(ERα$^+$) breast cancer cells.

TRPM2 and Proliferation

Both MCF-7(ERα$^+$) and HME cell growth were monitored by using the WST-8 assay. As shown in Figure 5A, siRNA/TRPM2 treated MCF-7(ERα$^+$) cells showed a significant inhibitory effect on proliferation compared to MCF-7(ERα$^+$) cells that were transfected with scrambled siRNA ($p < 0.05$). In contrast, siRNA/TRPM2 had no inhibitory effect on HME cells, suggesting that knocking down TRPM2 does not inhibit cell growth in HME cells. In addition to its impact on proliferation, TRPM2 siRNA also caused significant morphological changes in the two cell types. After treatment with siRNA/TRPM2, MCF-7(ERα$^+$) cells appeared irregularly shaped, exhibiting fragmented plasma membranes (Figure 5B(b)). However, neither

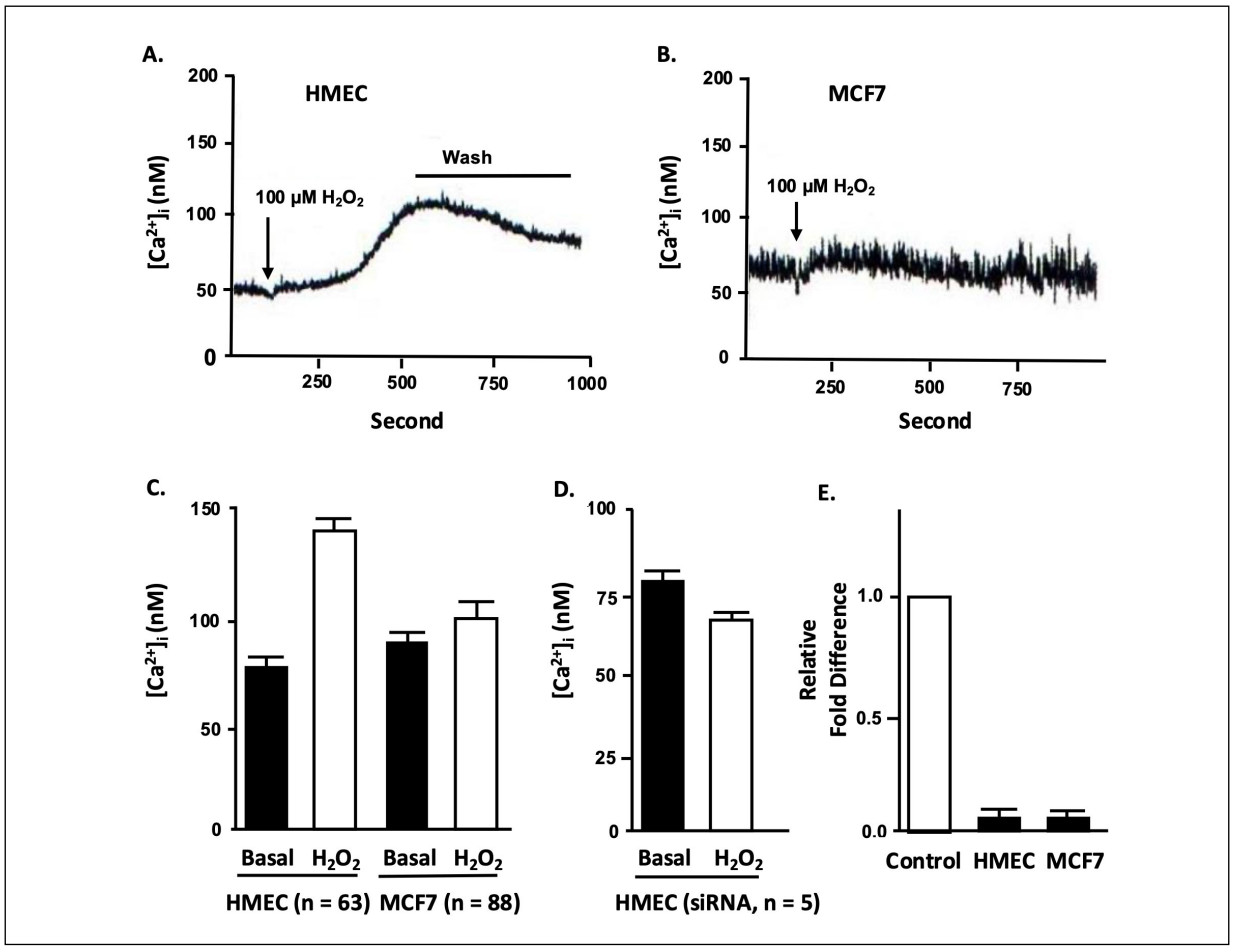

Figure 4. H_2O_2 induced elevation of intracellular calcium in HME cells and MCF-7(ERα$^+$) cells (as MCF-7). $[Ca^{2+}]_i$ was measured by a Fura-2 fluorescence ratio of 340 and 380 nm. *A* and *B*, changes in intracellular calcium after applying 100 μM H_2O_2 to HME cells and MCF-7(ERα$^+$) cells, respectively. *C*, pooled data from the two cell types before (solid bars) and after (open bars) H_2O_2 stimulation. *D*, HME cells treated with siRNA/TRPM2 for 48 hours. *E*, TRPM2 expression in HME cells and MCF-7(ERα$^+$) cells before (white bars) and after (black bars) treatment of 100 pM siRNA/TRPM for 48 hours. n = 3. * = $p < 0.01$.

MCF-7(ERα$^+$) cells treated with scrambled siRNA (Figure 5B(c)) nor HME cells treated with siRNA/TRPM2 5B[d] presented similar morphological characteristics.

Since the "knocking down" TRPM2 message had a detrimental effect on MCF-7(ERα$^+$) cell proliferation and morphology, we wanted to know whether siRNA/TRPM2 treatment resulted in cell apoptosis. Figure 6A(b) shows that many apoptotic MCF-7(ERα$^+$) cells were observed after 48 hours of treatment with siRNA/TRPM2. This effect was not observed in MCF-7(ERα$^+$) cells treated with scrambled siRNA (Figure 6A(c)) or in HME cells treated with siRNA/TRPM2 (Figure 6A(d)). Since the TUNEL assay was performed before significant cell death, our results may indicate early-stage apoptosis in these cells[32]. However, this does not rule out the possible occurrence of mid to late-stage necrosis. Figure 6B represents pooled data from the TUNEL assay showing a significant increase in apoptosis in MCF-7(ERα$^+$) cells treated with siRNA/TRPM2 compared to both untreated MCF-7 cells and siRNA/TRPM2 treated HME cells.

DISCUSSION

As the second most lethal form of cancer diagnosed in women in the United States, the death rate is 40% higher in NHB women than in NHW (28.4 *vs*. 20.3 deaths per 100,000 women). This death rate would double if NHB women were diagnosed with breast cancer at an age younger than 50 years old[33]. Also, the study used the Surveillance, Epidemiology, and End Results (SEER) data found a significant

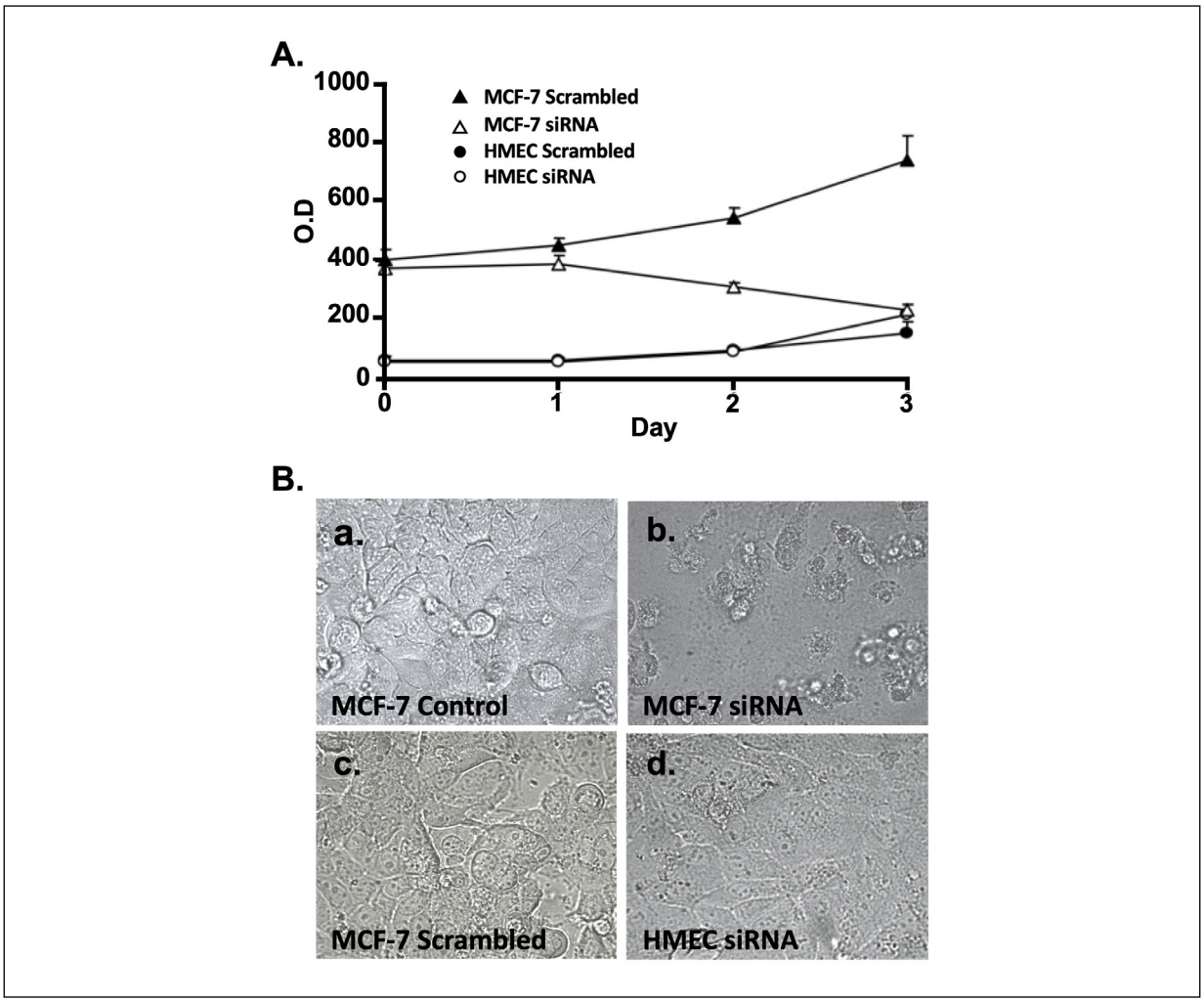

Figure 5. The proliferative and morphological effects of siRNA treatment on MCF-7 cells. *A*, the selective inhibitory effect of siRNA/TRPM2 (100 pM) treatment on cancer cell proliferation. Open circles represent cells treated with siRNA/TRPM2; solid circles represent cells treated with scrambled siRNA; Open triangles represent cells treated with siRNA/TRPM2; solid triangles represent cells treated with scrambled siRNA. Error = SD, n = 4. *B(a)*, control MCF-7(ERα^+) cells. *B(b)*, MCF-7(ERα^+) cells treated with siRNA/TRPM2 for 48 hrs; *B(c)*, MCF-7(ERα^+) cells treated with scrambled siRNA for 48 hrs; *B(d)*, HMEC treated with siRNA/TRPM2 for 48 hrs.

increase in second breast tumors in NHB with ductal carcinoma *in situ* (Relative Risk (RR): 1.25, 95% Confidence Interval: 1.08-1.36) when compared to NHW[34]. Additionally, NHB women have a significantly higher risk of developing invasive breast cancer after lobular carcinoma *in situ*[35]. To address these significant racial disparities, it is necessary to identify more racial-specific and stage-sensitive breast cancer proteins and to reveal these proteins' pathological mechanisms in the breast cancer progression in NHB and NHW women. The results presented in this study suggest that TRPM2 protein might be an important functional protein involved in the progression of breast cancer and might play a role in the racial disparity of the disease.

Generally, TRPM2 cation channels are expressed primarily in the plasma membrane and play a key role in oxidative stress-induced cell death[36]. Our results reveal a different role of the TRPM2 channel protein in cancer cells. It appears that these proteins facilitate or promote cell survival and proliferation while at the same time preventing the cells from being susceptible to oxidative stress-induced cell death. The molecular mechanism behind this altered function in cancer cells remains elusive.

In non-cancerous HME cells, TRPM2 channels are located on the plasma membrane, mediating calcium influx upon oxidative stimulation. We have demonstrated a significant change in the subcellular distribution of the TRPM2 protein in breast carcinoma MCF-7(ERα^+) cells where TRPM2's role as an ion channel is less critical due to the internalization and nuclear-localization of TRPM2 as shown in Figure

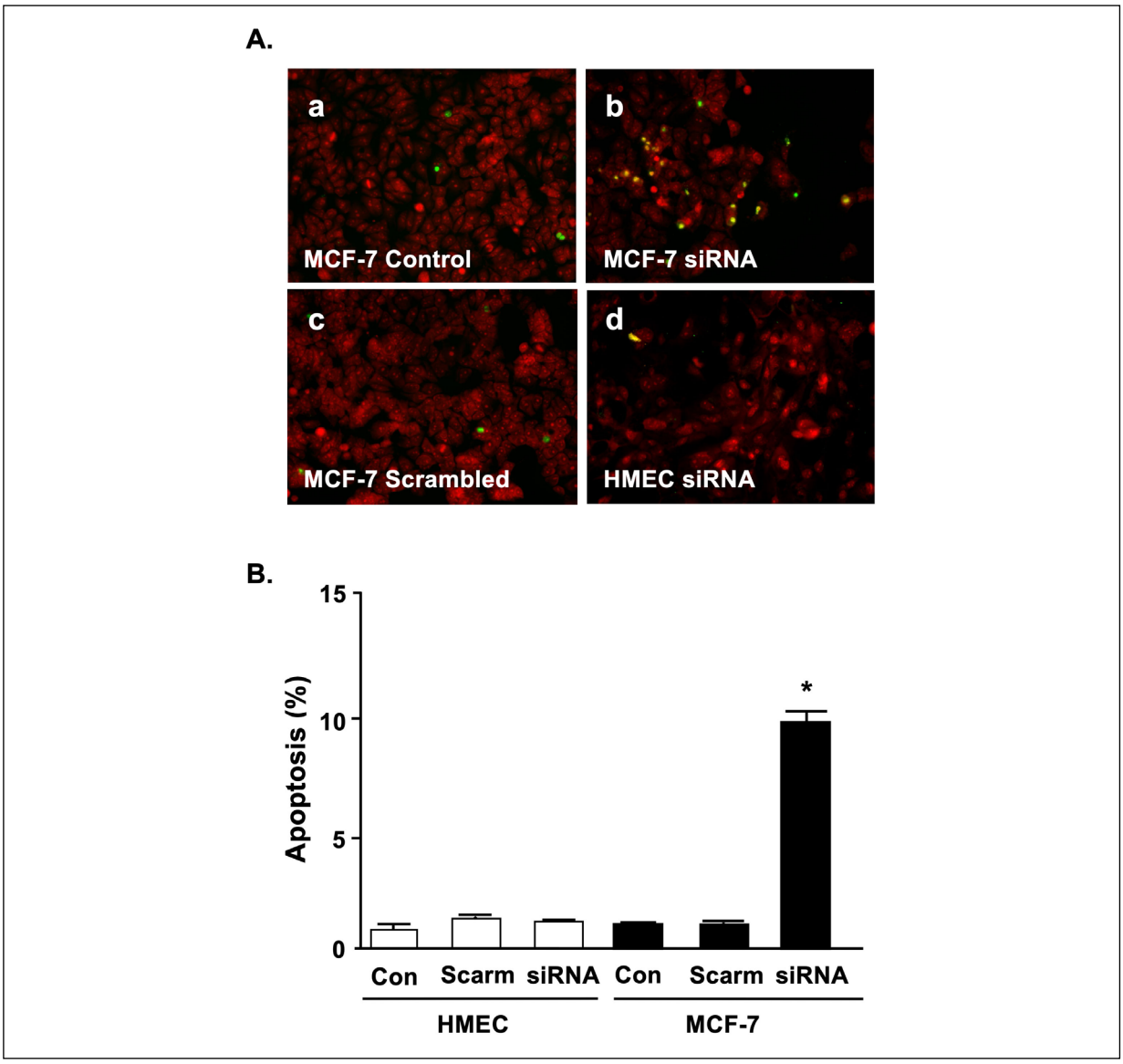

Figure 6. Apoptosis induced by siRNA/TRPM2 in MCF-7(ERα⁺) cells. *A*(a), controls MCF-7(ERα⁺) cells. *A*(b), MCF-7(ERα⁺) cells treated with siRNA/TRPM2 for 48 hrs. *A*(c), MCF-7(ERα⁺) cells treated with scrambled siRNA for 48 hrs. *A*(d), HMEC treated with siRNA/TRPM2 for 48 hrs. Red represents PI-labeled nuclei. Green/yellow represents labeled fluorescein nucleotide tagging of DNA fragments. *B*, percentage of apoptotic cells from combined data, $p < 0.01$, n = 3.

2B. In this case, most TRPM2 proteins appear to be translocated into the cytoplasm and nucleus, where they may play an enzymatic role in facilitating DNA synthesis or cell division.

The concept of this protein serving an enzymatic role is noticeable. TRPM2 contains a Nudix box in its C terminus[13], a common motif of enzymes that degrade nucleotide diphosphates and provide a binding site for ADP-ribose. ADP-ribose in the nucleus is converted into poly(ADP-ribose) by poly(ADP-ribose) polymerase (PARP), which plays a vital role in DNA repair[19] and cell replication[22]. Over-activation of PARP can cause cell necrosis due to the depletion of the cytoplasmic ATP[25]. TRPM2 can also catalyze mono-ADP-ribosylation and produce nonenzymatic ADP-ribosylation on target proteins[37,38]. An increased nuclear expression of TRPM2 directly or indirectly may affect the poly-ADP-ribosylation level. Precise control over poly-ADP-ribosylation may be crucial for cancer cell proliferation since highly activated PARP has been reported in malignant tumors[39,40]. If not restrained, overactive PARP could be detrimental to the survival of the cells.

Additionally, TRPM2 may play a crucial role in the dysregulation of cancer cell metabolism. In coordination with the need for increased energy utilization, cancer-induced metabolic changes alter the epigenetic landscape, including histone acetylation[41]. Histone acetyltransferases (HATS) deliver an acetyl group from acetyl-CoA to histone[42], whereas SIRT-family histone deacetylases catalyze the reverse reaction via an NAD^+-dependent mechanism[43]. Over-expression of TRPM2 in the nucleus may drain the NAD^+ by binding NAD^+ or ADPR to the NUDT-9 domain[13]. Decreased NAD^+ and histone deacetylation will promote malignant transformation and cell progression[44].

CONCLUSIONS

TRPM2 expression in the nucleus of breast cancer cells correlates with the cell's resistance to oxidative stimuli and appears to be an important factor in cancer cell survival. A key to understanding how the protein conveys a protective role in these cells must include understanding the mechanisms involved in TRPM2 transmigration to the nucleus. Since TRPM2 does not contain a nuclear localization signaling sequence, chaperone proteins may be involved in TRPM2 translocation. It has been previously shown that the inositol 1,4,5-trisphosphate receptor (IP_3R) can migrate into the nucleus and that IP_3R directly binds to TRPC (canonical) channels[45,46]. A similar intracellular trafficking mechanism could also be present for TRPM2. Another critical aspect in understanding TRPM2's role in cancer cell proliferation requires more investigation into the relationship between PARP and TRPM2 activity.

Ethical Approval:

Not Applicable

Consent for Publication:

All authors read and approved the final manuscript.

Data Availability Statements:

All the non-human data included in this study are available upon request by contact with the corresponding author. All human-normalized mRNA expression data was accessed from an online public database.

Funding:

NSF pilot pFund. "Title: Altered pattern of TRPM2 expression in human breast and prostate tumor tissues".

Author Contribution:

LH and ML designed the research. LH performed all benchwork work. YL completed public data analysis. LH, YL, and ML wrote the manuscript.

ORCID ID:

Luping Huang: 0009-0009-1692-640X
You Lu: 0000-0002-6815-6568
Ming Li: 0000-0001-6675-4903

Declaration of Conflicting Interests:

The author(s) declared no potential conflicts of interest with respect to the research, authorship, and/or publication of this article.

REFERENCES

1. Newman LA. Breast cancer in African-American women. Oncologist 2005; 10: 1-14.
2. Amirikia KC, Mills P, Bush J, Newman LA. Higher population-based incidence rates of triple-negative breast cancer among young African-American women: implications for breast cancer screening recommendations. Cancer 2011; 117: 2747-2753.

3. Cocco S, Piezzo M, Calabrese A, Cianniello D, Caputo R, Lauro VD, Fusco G, Gioia GD, Licenziato M, De Laurentiis M. Biomarkers in Triple-Negative Breast Cancer: State-of-the-Art and Future Perspectives. Int J Mol Sci 2020; 21: 4579.
4. Missiaen L, Robberecht W, van den Bosch L, Callewaert G, Parys JB, Wuytack F, Raeymaekers L, Nilius B, Eggermont J, De Smedt H. Abnormal intracellular ca(2+)homeostasis and disease. Cell Calcium 2000; 28: 1-21.
5. Miller BA. TRPM2 in Cancer. Cell Calcium 2019; 80: 8-17.
6. Ali ES, Chakrabarty B, Ramproshad S, Mondal B, Kundu N, Sarkar C, Sharifi-Rad J, Calina D, Cho WC. TRPM2-mediated Ca^{2+} signaling as a potential therapeutic target in cancer treatment: an updated review of its role in survival and proliferation of cancer cells. Cell Commun Signal 2023; 21: 145.
7. Hara Y, Wakamori M, Ishii M, Maeno E, Nishida M, Yoshida T, Yamada H, Shimizu S, Mori E, Kudoh J, Shimizu N, Kurose H, Okada Y, Imoto K, Mori Y. LTRPC2 Ca^{2+}-permeable channel activated by changes in redox status confers susceptibility to cell death. Mol Cell 2002; 9: 163-173.
8. Wehage E, Eisfeld J, Heiner I, Jüngling E, Zitt C, Lückhoff A. Activation of the cation channel long transient receptor potential channel 2 (LTRPC2) by hydrogen peroxide. A splice variant reveals a mode of activation independent of ADP-ribose. J Biol Chem 2002; 277: 23150-23156.
9. Perraud AL, Schmitz C, Scharenberg AM. TRPM2 Ca^{2+} permeable cation channels: from gene to biological function. Cell Calcium 2003; 33: 519-531.
10. Wang L, Fu TM, Zhou Y, Xia S, Greka A, Wu H. Structures and gating mechanism of human TRPM2. Science 2018; 362: eaav4809.
11. Hofmann T, Schaefer M, Schultz G, Gudermann T. Cloning, expression and subcellular localization of two novel splice variants of mouse transient receptor potential channel 2. Biochem J 2000; 351(Pt 1): 115-122.
12. Huang Y, Winkler PA, Sun W, Lü W, Du J. Architecture of the TRPM2 channel and its activation mechanism by ADP-ribose and calcium. Nature 2018; 562: 145-149.
13. Perraud AL, Fleig A, Dunn CA, Bagley LA, Launay P, Schmitz C, Stokes AJ, Zhu Q, Bessman MJ, Penner R, Kinet JP, Scharenberg AM. ADP-ribose gating of the calcium-permeable LTRPC2 channel revealed by Nudix motif homology. Nature 2001; 411: 595-599.
14. Tong Q, Zhang W, Conrad K, Mostoller K, Cheung JY, Peterson BZ, Miller BA. Regulation of the transient receptor potential channel TRPM2 by the Ca^{2+} sensor calmodulin. J Biol Chem 2006; 281: 9076-9085.
15. Kraft R, Grimm C, Grosse K, Hoffmann A, Sauerbruch S, Kettenmann H, Schultz G, Harteneck C. Hydrogen peroxide and ADP-ribose induce TRPM2-mediated calcium influx and cation currents in microglia. Am J Physiol Cell Physiol 2004; 286: C129-137.
16. Clapham DE. TRP channels as cellular sensors. Nature. 2003;426:517-524.
17. Kühn FJ, Lückhoff A. Sites of the NUDT9-H domain critical for ADP-ribose activation of the cation channel TRPM2. J Biol Chem 2004; 279: 46431-46437.
18. Rafty LA, Schmidt MT, Perraud AL, Scharenberg AM, Denu JM. Analysis of O-acetyl-ADP-ribose as a target for Nudix ADP-ribose hydrolases. J Biol Chem. 2002; 277: 47114-47122.
19. Shall S, de Murcia G. Poly(ADP-ribose) polymerase-1: what have we learned from the deficient mouse model? Mutat Res 2000; 460: 1-15.
20. Javle M, Curtin NJ. The role of PARP in DNA repair and its therapeutic exploitation. Br J Cancer 2011; 105: 1114-1122.
21. Pascal JM. The comings and goings of PARP-1 in response to DNA damage. DNA Repair (Amst) 2018; 71: 177-182.
22. Virág L, Szabó C. The therapeutic potential of poly(ADP-ribose) polymerase inhibitors. Pharmacol Rev 2002; 54: 375-429.
23. Virág L, Szabó C. The therapeutic potential of poly(ADP-ribose) polymerase inhibitors. Pharmacol Rev 2002; 54: 375-429.
24. Gibson BA, Kraus WL. New insights into the molecular and cellular functions of poly(ADP-ribose) and PARPs. Nat Rev Mol Cell Biol 2012; 13: 411-424.
25. Schreiber V, Hunting D, Trucco C, Gowans B, Grunwald D, De Murcia G, De Murcia JM. A dominant-negative mutant of human poly(ADP-ribose) polymerase affects cell recovery, apoptosis, and sister chromatid exchange following DNA damage. Proc Natl Acad Sci U S A 1995; 92: 4753-4757.
26. Kleczkowska HE, Althaus FR. The role of poly(ADP-ribosyl)ation in the adaptive response. Mutat Res 1996; 358: 215-221.
27. Fonfria E, Marshall IC, Benham CD, Boyfield I, Brown JD, Hill K, Hughes JP, Skaper SD, McNulty S. TRPM2 channel opening in response to oxidative stress is dependent on activation of poly(ADP-ribose) polymerase. Br J Pharmacol 2004; 143: 186-192.
28. Buelow B, Song Y, Scharenberg AM. The Poly(ADP-ribose) polymerase PARP-1 is required for oxidative stress-induced TRPM2 activation in lymphocytes. J Biol Chem 2008; 283: 24571-24583.
29. Naziroğlu M. New molecular mechanisms on the activation of TRPM2 channels by oxidative stress and ADP-ribose. Neurochem Res 2007; 32: 1990-2001.
30. Güzel M, Nazıroğlu M, Akpınar O, Çınar R. Interferon Gamma-Mediated Oxidative Stress Induces Apoptosis, Neuroinflammation, Zinc Ion Influx, and TRPM2 Channel Activation in Neuronal Cell Line: Modulator Role of Curcumin. Inflammation 2021; 44: 1878-1894.
31. Zhang W, Hirschler-Laszkiewicz I, Tong Q, Conrad K, Sun SC, Penn L, Barber DL, Stahl R, Carey DJ, Cheung JY, Miller BA. TRPM2 is an ion channel that modulates hematopoietic cell death through activation of caspases and PARP cleavage. Am J Physiol Cell Physiol 2006; 290: C1146-C1159.
32. Eisfeld J, Lückhoff A. Trpm2. In: Veit Flockerzi, Bernd Nilius. Transient Receptor Potential (TRP) Channels. Springer Nature, 2007; pp. 237-252.
33. DeSantis CE, Ma J, Gaudet MM, Newman LA, Miller KD, Goding Sauer A, Jemal A, Siegel RL. Breast cancer statistics, 2019. CA Cancer J Clin 2019; 69: 438-451.
34. Liu Y, Colditz GA, Gehlert S, Goodman M. Racial disparities in risk of second breast tumors after ductal carcinoma *in situ*. Breast Cancer Res Treat 2014; 148: 163-173.
35. Dania V, Liu Y, Ademuyiwa F, Weber JD, Colditz GA. Associations of race and ethnicity with risk of developing invasive breast cancer after lobular carcinoma *in situ*. Breast Cancer Res 2019; 21: 120.
36. Zhang W, Chu X, Tong Q, Cheung JY, Conrad K, Masker K, Miller BA. A novel TRPM2 isoform inhibits calcium influx and susceptibility to cell death. J Biol Chem 2003; 278: 16222-16229.
37. Ziegler M, Niere M. NAD_+ surfaces again. Biochem J 2004; 382(Pt 3): e5-6.

38. Okuda K, Hayashi H, Nishiyama Y. Systematic characterization of the ADP-ribose pyrophosphatase family in the Cyanobacterium Synechocystis sp. strain PCC 6803. J Bacteriol 2005; 187: 4984-4991.
39. Hirai K, Ueda K, Hayaishi O. Aberration of poly(adenosine diphosphate-ribose) metabolism in human colon adenomatous polyps and cancers. Cancer Res 1983; 43: 3441-3446.
40. M. Shiobara, M. Miyazaki, H. Ito, A. Togawa, N. Nakajima, F. Nomura, N. Morinaga, and M. Shiobara M, Miyazaki M, Ito H, Togawa A, Nakajima N, Nomura F, Morinaga N, Noda M. Enhanced polyadenosine diphosphate-ribosylation in cirrhotic liver and carcinoma tissues in patients with hepatocellular carcinoma. J Gastroenterol Hepatol 2001; 16: 338-344.
41. Wang YP, Lei QY. Metabolic recoding of epigenetics in cancer. Cancer Commun (Lond) 2018; 38: 25.
42. Roth SY, Denu JM, Allis CD. Histone acetyltransferases. Annu Rev Biochem 2001; 70: 81-120.
43. Sosnowska B, Mazidi M, Penson P, Gluba-Brzózka A, Rysz J, Banach M. The sirtuin family members SIRT1, SIRT3 and SIRT6: Their role in vascular biology and atherogenesis. Atherosclerosis 2017; 265: 275-282.
44. Patra S, Panigrahi DP, Praharaj PP, Bhol CS, Mahapatra KK, Mishra SR, Behera BP, Jena M, Bhutia SK. Dysregulation of histone deacetylases in carcinogenesis and tumor progression: a possible link to apoptosis and autophagy. Cell Mol Life Sci 2019; 76: 3263-3282.
45. Boulay G, Brown DM, Qin N, Jiang M, Dietrich A, Zhu MX, Chen Z, Birnbaumer M, Mikoshiba K, Birnbaumer L. Modulation of Ca(2+) entry by polypeptides of the inositol 1,4, 5-trisphosphate receptor (IP3R) that bind transient receptor potential (TRP): evidence for roles of TRP and IP3R in store depletion-activated Ca(2+) entry. Proc Natl Acad Sci U S A 1999; 96: 14955-14960.
46. Zhu MX, Tang J. TRPC channel interactions with calmodulin and IP3 receptors. Novartis Found Symp 2004; 258: 44-58; discussion 58-62, 98-102, 263-266.